

## Accepted Manuscript

Rational design and synthesis of 2-anilinopyridinyl-benzothiazole Schiff bases as antimitotic agents

Thokhir B. Shaik, S.M. Ali Hussaini, V. Lakshma Nayak, M. Lakshmi  
Sucharitha, M. Shaheer Malik, Ahmed Kamal

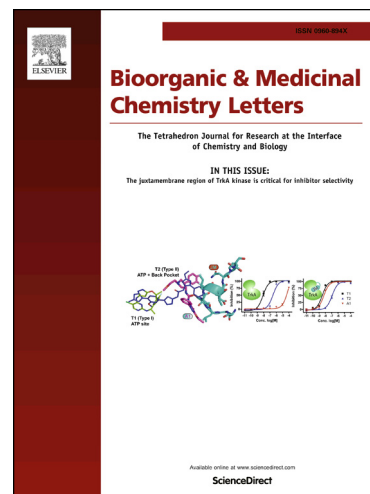
PII: S0960-894X(17)30337-2  
DOI: <http://dx.doi.org/10.1016/j.bmcl.2017.03.089>  
Reference: BMCL 24841

To appear in: *Bioorganic & Medicinal Chemistry Letters*

Received Date: 3 October 2016  
Revised Date: 27 March 2017  
Accepted Date: 29 March 2017

Please cite this article as: Shaik, T.B., Hussaini, S.M.A., Nayak, V.L., i Sucharitha, M.L., Malik, M.S., Kamal, A., Rational design and synthesis of 2-anilinopyridinyl-benzothiazole Schiff bases as antimitotic agents, *Bioorganic & Medicinal Chemistry Letters* (2017), doi: <http://dx.doi.org/10.1016/j.bmcl.2017.03.089>

This is a PDF file of an unedited manuscript that has been accepted for publication. As a service to our customers we are providing this early version of the manuscript. The manuscript will undergo copyediting, typesetting, and review of the resulting proof before it is published in its final form. Please note that during the production process errors may be discovered which could affect the content, and all legal disclaimers that apply to the journal pertain.



## Rational design and synthesis of 2-anilinopyridinyl-benzothiazole Schiff bases as antimitotic agents

Thokhir B. Shaik,<sup>a,c,§</sup> S. M. Ali Hussaini,<sup>a,d,§</sup> V. Lakshma Nayak,<sup>a</sup> M. Lakshmi Sucharitha,<sup>b</sup> M. Shaheer Malik,<sup>a,c</sup> Ahmed Kamal<sup>\*a,b</sup>

<sup>a</sup>Medicinal Chemistry and Pharmacology, CSIR – Indian Institute of Chemical Technology, Hyderabad 500 007, India; <sup>b</sup>Department of Medicinal Chemistry, National Institute of Pharmaceutical Education & Research (NIPER), Hyderabad 500 037, India.

<sup>c</sup>Department of Biotechnology, Acharya Nagarjuna University, Nagarjuna Nagar, Guntur 522510, India

<sup>d</sup>Present address: Department of Chemistry, University of Saskatchewan, 110 Science Place, Saskatoon, SK S7N 5C9, Canada

<sup>e</sup>Present address: Science and Technology Unit, Umm Al-Qura University, Makkah, Saudi Arabia.

<sup>§</sup>Contributed equally.

**Abstract:** Based on our previous results and literature precedence, a series of 2-anilinopyridinyl-benzothiazole Schiff bases were rationally designed by performing molecular modelling experiments on some selected molecules. The binding energies of the docked molecules were better than the E7010, and the Schiff base with trimethoxy group on benzothiazole moiety, **4y** was the best. This was followed by the synthesis of a series of the designed molecules by a convenient synthetic route and evaluation of their anticancer potential. Most of the compounds have shown significant growth inhibition against the tested cell lines and the compound **4y** exhibited good antiproliferative activity with a GI<sub>50</sub> value of 3.8 μM specifically against the cell line DU145. In agreement with the docking results, **4y** exerted cytotoxicity by the disruption of the microtubule dynamics by inhibiting tubulin polymerization via effective binding into colchicine domain, comparable to E7010. Detailed binding modes of **4y** with colchicine binding site of tubulin were studied by molecular docking. Furthermore, **4y** induced apoptosis as evidenced by biological studies like mitochondrial membrane potential, caspase-3, and Annexin V-FITC assays.

---

**Keywords:** E7010, Benzothiazole, Cytotoxicity, Cell cycle, Tubulin polymerization.

<sup>\*a,b</sup>Corresponding authors. Tel.: +91-40-27193157; fax: +91-40-27193189 (A.K.); e-mail: [ahmedkamal@iict.res.in](mailto:ahmedkamal@iict.res.in) (A. Kamal).

Mitosis is the last stage of cell cycle characterized by splitting of a parent cell into two daughter cells. This process is aided by microtubules which are key components of the cytoskeleton in eukaryotic cells.<sup>1</sup> Microtubules play a crucial role in several cellular processes, one of which include playing out from opposite ends of the cell thereby pulling the sister chromatids of each chromosome apart leading to cell division.<sup>2</sup> These are long, filamentous, tube-shaped structures formed by the polymerization of  $\alpha$ ,  $\beta$ -tubulin heterodimers. Microtubules are highly dynamic polymers that dissociate to tubulin heterodimers and associate back to form microtubules.<sup>3</sup> Any perturbation in these dynamics results in a programmed cell death and this provides a scope for the development of anticancer agents. Moreover, microtubules are also reported to play a significant role in angiogenesis, a process by which new blood vessels are formed, providing nutrients (blood) to the tumor. Interestingly, microtubule-targeting agents demonstrated antiangiogenic effects cutting off the blood supply by disrupting tumor vasculature at substantially lower concentrations than those at which antimetabolic effect is observed.<sup>4</sup> Therefore, targeting microtubules is a validated approach for cancer drug development. As tubulin is the main component of microtubules, compounds inhibiting tubulin intervene with microtubule dynamics and arrest the cell cycle in the G<sub>2</sub>/M phase leading to apoptosis. Among the four well known binding sites on tubulin, colchicine binding site named after naturally occurring colchicine (**1**) is one of the extensively studied targets for developing tubulin polymerization inhibitors.<sup>5</sup> However, in recent past, quite a few molecules structurally distinct from colchicine have been crystallized in the colchicine binding site. The sulphonamide E7010 (**2**), is an orally bioavailable tubulin binding agent that exerts cytotoxic effects by binding to the colchicine binding site.<sup>6</sup> It is reported to possess a wide spectrum of antitumor activity and is even effective against certain multidrug resistant cells. Comparative structural analysis of E7010 binding to colchicine binding site of tubulin indicates that its sulphonamide bridge overlaps with the B ring while the pyridine and methoxy groups superimpose with A and C rings of the colchicine respectively.

On the other hand, benzothiazole is a privileged heterocyclic scaffold with diverse biological properties including anticancer activity.<sup>7</sup> Several structurally simple benzothiazoles are reported to possess excellent *in vitro* and *in vivo* cytotoxicity at low nanomolar concentrations. Phortress (**3**), a prodrug is one of the best examples of such drug candidates presently undergoing phase I clinical trials.<sup>8</sup> Moreover, it is evident from the literature that a large number of molecules

possessing potential anticancer activity are the outcome of modifications done on the benzothiazole scaffold. Therefore, based on our previous work on the development of newer anticancer agents based on E7010<sup>10</sup> as well as benzothiazole structures,<sup>11</sup> a series of 2-anilinopyridinyl-benzothiazole Schiff bases were rationally designed by performing molecular docking experiments taking into account the pharmaceutical background of Schiff bases.<sup>12</sup> We herein report the synthesis and biological evaluation of these 2-anilinopyridinyl-benzothiazole Schiff bases (**4a-ad**), their ability to inhibit tubulin polymerization apart from inducing apoptosis.

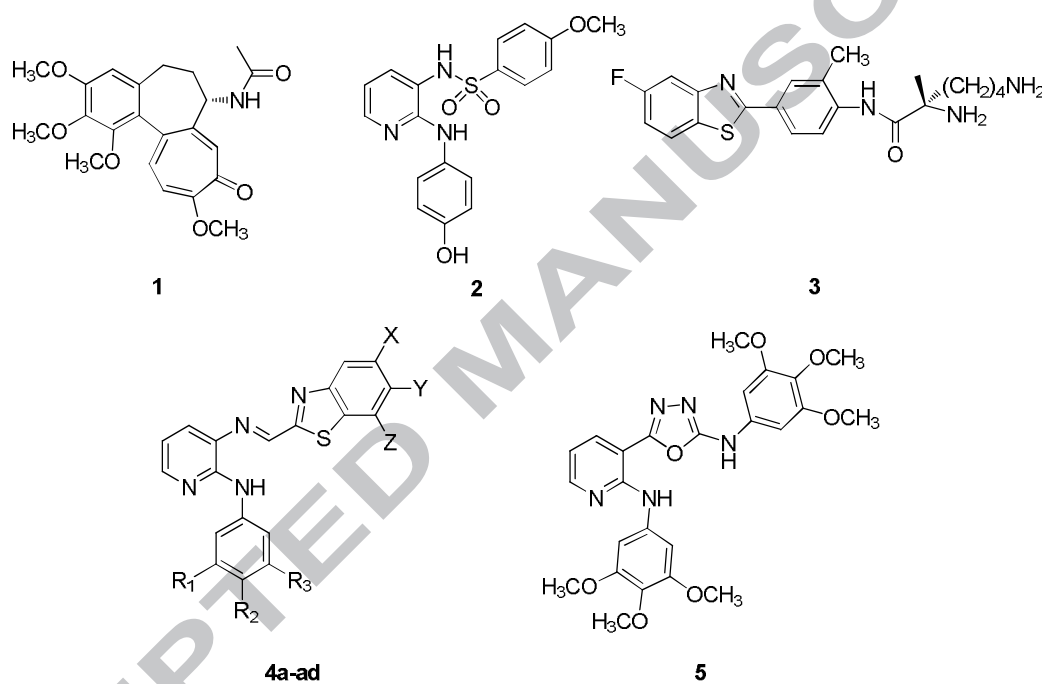


**Figure 1:** Anticancer agents.

In recent years, our research endeavors on the development of newer anticancer agents based on E7010 has produced fruitful results.<sup>10</sup> From the previous reports and experiences, we have observed that 2-anilinopyridine moiety of E7010 is crucial for the anticancer activity and attempts to cyclize the secondary amine was deleterious for the cytotoxic activity.<sup>13</sup> In this context, one of the 2-anilinopyridinyl-oxadiazole conjugates (compound **5**) developed in our laboratory was found to be an effective inhibitor of tubulin polymerization.<sup>14</sup> Moreover in another effort, improved cytotoxicity was observed on conjugating benzothiazole and 2-anilinopyridine moieties via an amide functionality.<sup>15</sup> In continuation of our research in this area,

we have rationally designed a new molecular structure retaining 2-anilinopyridine moiety and replacing the amino oxadiazole core of **5** with imino thiazole fused to a benzene ring (Figure 2). The trimethoxy anilinopyridine was also retained as the trimethoxy group is known to show crucial interactive potential with microtubules.<sup>16</sup> The imine functionality as Schiff base, was selected taking into account the conformational flexibility it imparts, which is presumed to be helpful in efficiently interacting at the binding pocket of colchicine domain.<sup>12</sup>

## 2.1 Design:

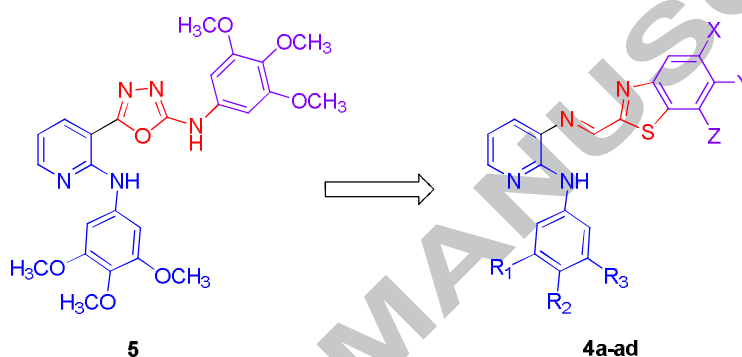


**Figure 2:** Strategy of the design.

In this regard, *in silico* molecular modeling studies have been carried out on certain structures obtained by tethering 2-trimethoxyanilinopyridine and benzothiazole moieties via an imine linkage. These structures with variable substituents on benzothiazole nucleus were docked into the colchicine binding site of tubulin. The protein structure of tubulin was downloaded from the protein data bank (PDB code: 3E22) and the docking studies were performed using the software Autodock 4.2.<sup>17</sup> Figures **3A**, **3B**, **3C**, and **3D** represent the binding modes of compounds possessing fluoro, chloro, methoxy and trimethoxy substituents on the benzothiazole with colchicine binding site of tubulin. As evident from these figures (**3A**, **3B**, and **3C**), compounds with fluoro, chloro and methoxy substituents on the benzothiazole interact with the protein by establishing two and one hydrogen bonding interactions each, respectively. Whereas the compound bearing trimethoxy substituent on benzothiazole establishes three hydrogen bonding interactions as shown in Figure **3D**. It is noteworthy that in the case of monosubstitution on benzothiazole, either benzothiazole or 2-anilinopyridine moiety is involved in the hydrogen bonding interaction. However, in the case of trimethoxy substituent, two out of the three

hydrogen bonding interactions are established by 2-anilinopyridine moiety while benzothiazole is involved in only one interaction (discussed in detail in molecular modeling section). This presupposition is supported by the binding energies of these molecules with the tubulin. Compounds with fluoro, chloro, methoxy and trimethoxy substituents have binding energies in the order -9.02, -9.20, -8.80, -9.26 kcal/mol, respectively. Interestingly, the standard molecule E7010, a known inhibitor of colchicine binding site shows a binding energy of -8.64 kcal/mol. Therefore, it was considered of interest to synthesize these conjugates along with related ones and study their biological profile experimentally.

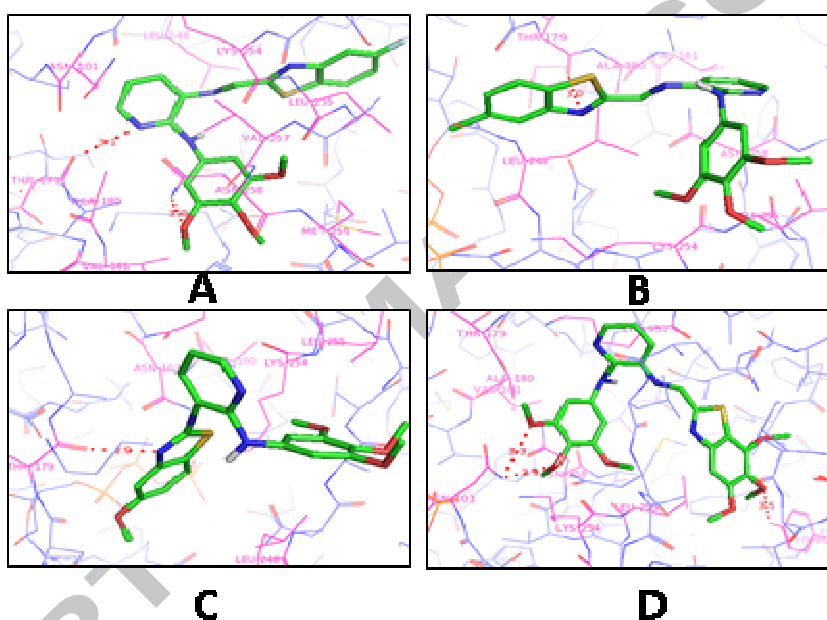
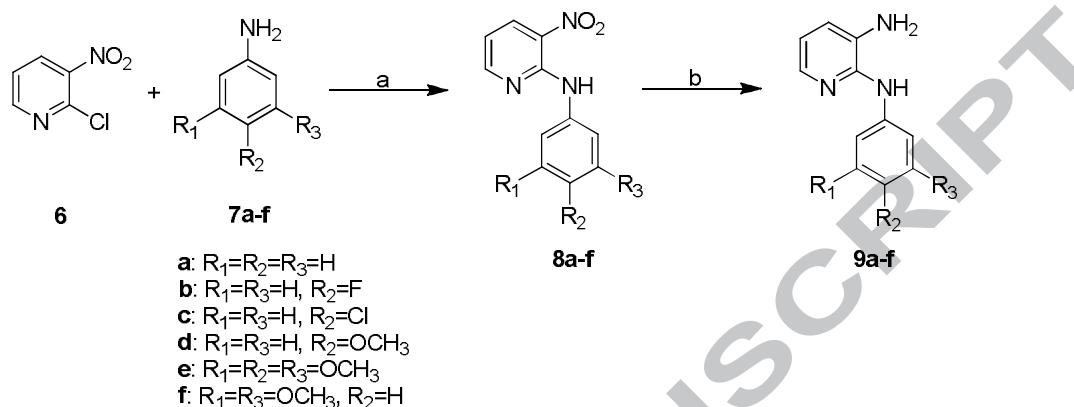


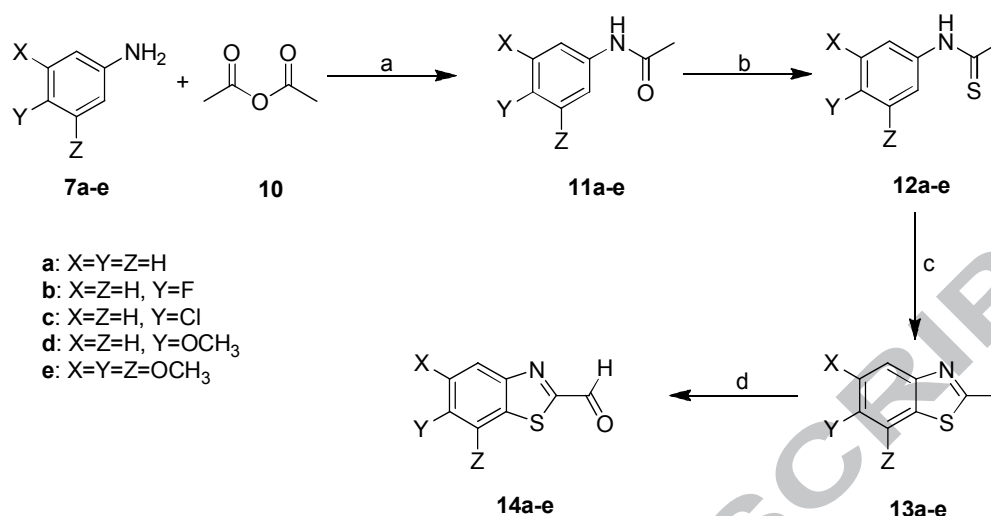
**Figure 3:** Binding modes of compounds **4g** (A), **4h** (B), **4x** (C) and **4y** (D) with colchicine binding site.

The aniline intermediates required for the synthesis of the final Schiff bases were obtained by following a convenient synthetic route outlined in Scheme 1. Commercially available 2-chloro-3-nitropyridine (**6**) was heated with substituted anilines (**7a-f**) in ethylene glycol at 140 °C for 8 hours. This aromatic nucleophilic substitution reaction yielded substituted 2-anilino-3-nitropyridines (**8a-f**). The substituents on anilines used for this reaction include fluoro, chloro, methoxy, dimethoxy and trimethoxy. Reduction of 2-anilino-3-nitropyridine derivatives with the help of reducing agent stannous chloride ( $\text{SnCl}_2 \cdot 2\text{H}_2\text{O}$ ) in methanol gave the amine precursors in good yields (**9a-f**).



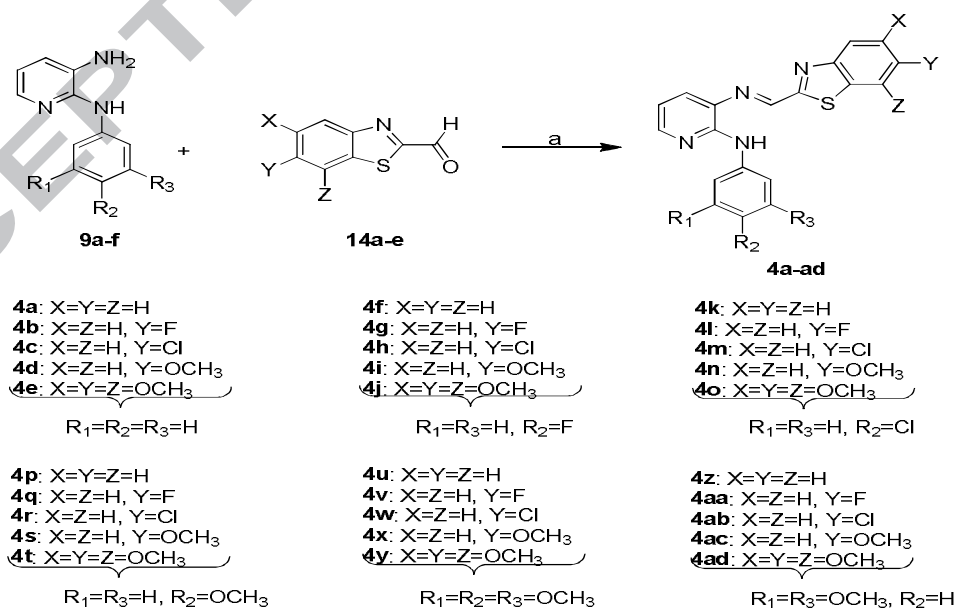
**Scheme 1.** Reagents and conditions: a) Ethylene glycol, 140 °C, 8 h; b)  $\text{SnCl}_2 \cdot 2\text{H}_2\text{O}$ , methanol, 80 °C, 3 h.

The aldehyde precursors were synthesized by following the synthetic route described in Scheme 2. Commercially available substituted anilines (**7a-e**) were acetylated using acetic anhydride (**10**) in dichloromethane ( $\text{CH}_2\text{Cl}_2$ ). Substituents of different nature such as fluoro, chloro, methoxy and trimethoxy along with neutral hydrogen were used on aniline to study their effect on anticancer activity. The acetanilides formed (**11a-e**) were converted to their thioacetylated product (**12a-e**) by heating with Lawesson's reagent in dioxane. The thioacetanilides were cyclized to substituted 2-methylbenzothiazole derivatives (**13a-e**) via Jacobsen cyclization procedure i.e., by charging sodium hydroxide solution of thioacetanilides into preheated aqueous potassium ferricyanide  $\text{K}_3\text{Fe}(\text{CN})_6$  solution. Subsequently, the 2-methylbenzothiazole derivatives (**13a-e**) were refluxed with the oxidizing agent selenium dioxide ( $\text{SeO}_2$ ) in dioxane to yield the aldehyde precursors (**14a-e**) in significant yields.



**Scheme 2.** Reagents and conditions: a) CH<sub>2</sub>Cl<sub>2</sub>, rt, 15 mins; b) Lawesson's Reagent, dioxane, 110 °C, 2 h; c) K<sub>3</sub>Fe(CN)<sub>6</sub>, 8N NaOH, 80 °C, 0.5 h; d) SeO<sub>2</sub>, dioxane, 110 °C, 12 h.

With both the amine and aldehyde fragments in hand, the synthesis of target Schiff bases was achieved in a convenient manner as described in Scheme 3. The amine precursors (**8a-f**) obtained from Scheme 1 and aldehyde precursors (**13a-e**) prepared according to the Scheme 2 were condensed in ethanol at room temperature to afford the diversely substituted desired compounds (Schiff bases) in good yields (**4a-ad**).



**Scheme 3.** Reagents and conditions: a) Ethanol, rt, 1-2 h.

These 2-anilinopyridinyl-benzothiazole Schiff bases were evaluated for their anticancer potential against three different human cancer cell lines, namely A549, DU145, and MCF7. Cancer cells were seeded in 96 well plate at a density of  $2.5 \times 10^4$  cells per well. All the compounds were tested against each cell line at various concentrations namely 0.1, 1, 5 and 10  $\mu\text{M}$  and their growth inhibitory effects were determined by Sulforhodamine B assay after 48 h. Sulphonamide E7010 along with the standard drug 5-fluorouracil (5-FU) were taken as positive controls. From the growth inhibition data,  $\text{GI}_{50}$  values have been calculated which are tabulated in Table 1.

As seen from the data, 2-anilinopyridinyl-benzothiazole conjugates showed considerable cytotoxicity. The inhibitory effects due to these conjugates were observed to be of varied magnitude against these test cell lines. Some of these conjugates were found to be active below 20  $\mu\text{M}$  concentration, however some were not active even at 100  $\mu\text{M}$ . Interestingly, these conjugates have displayed specificity toward the prostate cancer cell line (DU145) and most of them have demonstrated significant cytotoxicities against it. Compound **4y** was the most potent conjugate of the series exhibiting significant to good antiproliferative activities against the cell lines A549, MCF 7 and DU145 with  $\text{GI}_{50}$  values of 17, 12 and 3.8  $\mu\text{M}$ , respectively. Similarly, compound **4t** was found to be an effective conjugate from the series displaying a  $\text{GI}_{50}$  of 4.3  $\mu\text{M}$  against the cell line A549. Moreover, other conjugates such as **4e**, **4h**, **4l**, **4s**, **4t** and **4w** have also exhibited significant antiproliferative activities against the corresponding cell lines. Further, these conjugates were evaluated for their cytotoxic effects on the normal human lung cells (MRC5). All the conjugates along with the standard were tested at various concentrations ranging from 1 to 100  $\mu\text{M}$  and the results demonstrated that all the conjugates showed no significant activity up to 100  $\mu\text{M}$  concentration except **4j** which showed the  $\text{GI}_{50}$  value of 91.1  $\mu\text{M}$ .

During the discussion in chemistry part, the various substituents used in the synthesis of 2-anilino pyridine and benzothiazole moieties of the desired Schiff bases have been described. The main objective of diversifying the final target structure is to study the effect of substituents on the anticancer activity. From the anticancer activity data shown in Table 1 it was analyzed that trimethoxy group on the benzothiazole nucleus is fruitful for cytotoxicity. In the presence of trimethoxy group on the benzothiazole moiety, both ring activating as well as deactivating

substituents at the 4th position of the aryl ring of 2-anilinopyridinyl moiety bestow significant cytotoxicity. This effect was observed in the absence of substituent also, but not for a 3,5-dimethoxy substituent. Effect of fluoro and chloro substituents on benzothiazole nucleus was also observed to be significant. These groups confer good cytotoxicity in the presence of ring deactivating substituents on 2-anilinopyridinyl moiety.

Compounds containing ring deactivating groups on 4th position of the aryl ring of 2-anilinopyridinyl moiety have demonstrated better antiproliferative effects than the compounds with ring activating substituents. Thus, fluoro and chloro groups on 4th position of the aryl ring of 2-anilinopyridinyl moiety are desirable while methoxy group at this position is not tolerable. However 3,5-dimethoxy substituent on 2-anilinopyridinyl confers significant activity. Interestingly the trimethoxy group, on both anilinopyridine and benzothiazole moiety, imparts most potent activity in comparison to others.

**Table 1:** Cytotoxic activity (<sup>a</sup>GI<sub>50</sub> in  $\mu\text{M}$ ) data of compounds, **4a-4ad** by SRB method.

Compd	<sup>a</sup> GI <sub>50</sub> values in $\mu\text{M}$			
	<sup>b</sup> A549	<sup>c</sup> MCF 7	<sup>d</sup> DU145	<sup>e</sup> MRC5
<b>4a</b>	N.A	85.1 $\pm$ 0.42	N.A	- <sup>f</sup>
<b>4b</b>	42.7 $\pm$ 0.36	N.A	N.A	- <sup>f</sup>
<b>4c</b>	N.A	56.5 $\pm$ 0.48	N.A	- <sup>f</sup>
<b>4d</b>	76.3 $\pm$ 0.28	32.9 $\pm$ 0.23	8.8 $\pm$ 0.11	- <sup>f</sup>
<b>4e</b>	N.A	12.4 $\pm$ 0.18	10.7 $\pm$ 0.14	- <sup>f</sup>
<b>4f</b>	N.A	10.7 $\pm$ 0.26	N.A	- <sup>f</sup>
<b>4g</b>	N.A	16.3 $\pm$ 0.15	N.A	- <sup>f</sup>
<b>4h</b>	14.2 $\pm$ 0.16	11.6 $\pm$ 0.22	16.6 $\pm$ 0.16	- <sup>f</sup>
<b>4i</b>	> 100	40.5 $\pm$ 0.31	N.A	- <sup>f</sup>
<b>4j</b>	12.3 $\pm$ 0.22	20.0 $\pm$ 0.29	25.2 $\pm$ 0.30	91.1 $\pm$ 0.5
<b>4k</b>	16.7 $\pm$ 0.18	17.7 $\pm$ 0.20	15.7 $\pm$ 0.35	- <sup>f</sup>
<b>4l</b>	N.A	31.4 $\pm$ 0.14	4.8 $\pm$ 0.24	- <sup>f</sup>
<b>4m</b>	8.6 $\pm$ 0.19	41.6 $\pm$ 0.43	12.7 $\pm$ 0.21	- <sup>f</sup>
<b>4n</b>	31.6 $\pm$ 0.26	N.A	N.A	- <sup>f</sup>
<b>4o</b>	12.4 $\pm$ 0.22	N.A	8.6 $\pm$ 0.36	- <sup>f</sup>
<b>4p</b>	11.1 $\pm$ 0.19	N.A	32.6 $\pm$ 0.48	- <sup>f</sup>
<b>4q</b>	N.A	N.A	18.9 $\pm$ 0.19	- <sup>f</sup>
<b>4r</b>	N.A	N.A	47.4 $\pm$ 0.24	- <sup>f</sup>
<b>4s</b>	5.8 $\pm$ 0.26	N.A	N.A	- <sup>f</sup>
<b>4t</b>	4.3 $\pm$ 0.17	N.A	12.5 $\pm$ 0.16	- <sup>f</sup>
<b>4u</b>	N.A	44.4 $\pm$ 0.22	N.A	- <sup>f</sup>

<b>4v</b>	N.A	N.A	10.8 ± 0.13	- <sup>f</sup>
<b>4w</b>	N.A	18.6 ± 0.16	7.9 ± 0.26	- <sup>f</sup>
<b>4x</b>	N.A	30.0 ± 0.52	20.7 ± 0.16	- <sup>f</sup>
<b>4y</b>	17.0 ± 0.18	12.0 ± 0.24	<b>3.8 ± 0.15</b>	- <sup>f</sup>
<b>4z</b>	N.A	15.1 ± 0.16	N.A	- <sup>f</sup>
<b>4aa</b>	18.9 ± 0.22	11.3 ± 0.22	N.A	- <sup>f</sup>
<b>4ab</b>	30.7 ± 0.28	21.8 ± 0.25	16.2 ± 0.18	- <sup>f</sup>
<b>4ac</b>	14.0 ± 0.26	19.9 ± 0.34	15.9 ± 0.24	- <sup>f</sup>
<b>4ad</b>	58.6 ± 0.49	19.8 ± 0.29	N.A	- <sup>f</sup>
E7010	1.31	1.53	1.81	- <sup>f</sup>
5-FU	2.09	1.67	5.82	- <sup>f</sup>

Note: <sup>a</sup> Concentration of drug causing 50% inhibition of cell growth, <sup>b</sup>A549- lung carcinoma cell line, <sup>c</sup>MCF 7- breast cancer cell line, <sup>d</sup>DU145- prostate cancer cell line, <sup>e</sup>MRC5 normal lung cells, <sup>-f</sup> GI50 values >100  $\mu$ M.

In order to understand the mechanism of action of Schiff base with two trimethoxy groups **4y**, the microtubule inhibitory ability was investigated and correlated with the docking results. The progression of tubulin polymerization<sup>18</sup> was thus examined by monitoring the absorbance at 340 nm in 384 well plate for 1 h at 37 °C with and without the conjugate at 3  $\mu$ M concentration in comparison with reference compound E7010. Thus compound (**4y**) significantly inhibited tubulin polymerization by 59.57 %, whereas the reference compound (E7010) exhibited 60.64 % inhibition (Figure 4). This was followed by evaluation of IC<sub>50</sub> values for this compound and the results are shown in Table 2. The test compound **4y** showed tubulin-assembly inhibition with an IC<sub>50</sub> value of 4.22  $\mu$ M, whereas the standard E7010 exhibited IC<sub>50</sub> of 2.51  $\mu$ M. The effect of these compounds on the inhibition of tubulin assembly correlated well with the *in silico* molecular modeling studies.

**Table 2:** Inhibition of tubulin polymerization (IC<sub>50</sub>) of compounds **4y** and E7010.

Compound	<sup>a</sup> IC <sub>50</sub> ± SD (in $\mu$ M)
<b>4y</b>	4.22 ± 0.13
E7010	2.51 ± 0.15

**Note:** <sup>a</sup> Concentration of drug to inhibit 50% of tubulin assembly.

### 3.2. Effect of compounds on tubulin polymerization

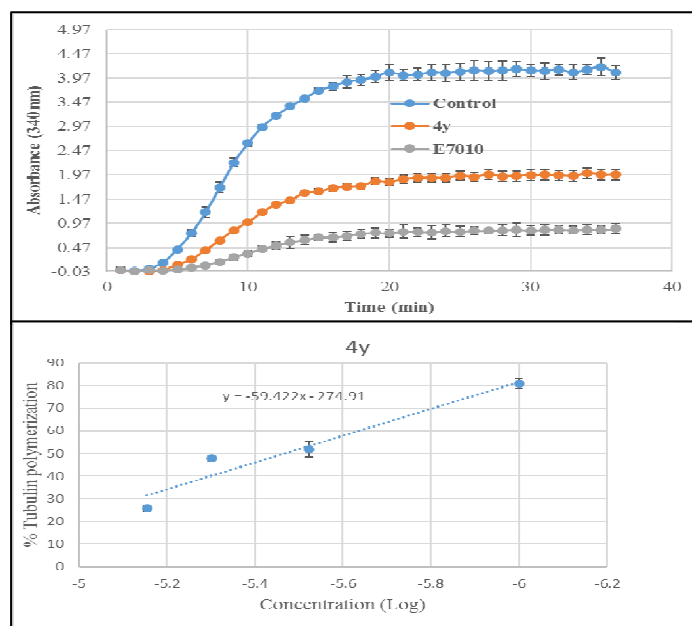


**Figure 4:** Effect of compound on tubulin polymerization: Tubulin polymerization was monitored by increase in absorbance at 340 nm for 1 h at 37 °C. E7010 was used as a positive control. Values indicated are the mean  $\pm$  SD of two different experiments performed in triplicates.

As conjugate **4y**, showed good inhibitory effects on tubulin polymerization similar to that of E7010 which is known to bind into colchicine binding site of the tubulin, it was considered of interest to investigate the binding of **4y** on this site of the tubulin. Hence, a fluorescence-based assay<sup>19</sup> was carried out taking E7010 as the positive control and vinblastine as the negative control. Thus **4y**, E7010 and vinblastine were separately coincubated with colchicine at 37 °C for 60 minutes and subsequently their fluorescence were measured. Figures 5A, 5B and 5C represent the scan of fluorescence wavelength for tubulin-colchicine complex from 600 to 390 nm fixing the excitation wavelength at 350 nm when coincubated with **4y**, E7010 and vinblastine respectively at various concentrations. From the Figures it is clear that the tubulin-colchicine complex gives fluorescence at 440 nm when excited at 350 nm, therefore the fluorescence was measured at the same wavelength. It is also noteworthy from the figures that **4y** and E7010 caused a significant decrease in the fluorescence whereas no such effect was observed in the case

of vinblastine. Similarly, Figure 5D represents the change in fluorescence intensity of tubulin-colchicine complex with the concentration of **4y**, E7010 and vinblastine. As evident from the figure, a significant decrease in the fluorescence was observed in the case of **4y** and E7010. However, vinblastine exerts no effect on the complex fluorescence as it binds at a different site on the tubulin. These observations indicate that **4y** and E7010 compete to bind to the tubulin at the colchicine binding site. Interestingly, **4y** caused greater lowering of the complex fluorescence than E7010 indicating that it is an effective inhibitor of colchicine binding site.

### 3.3. Competitive colchicine binding assay

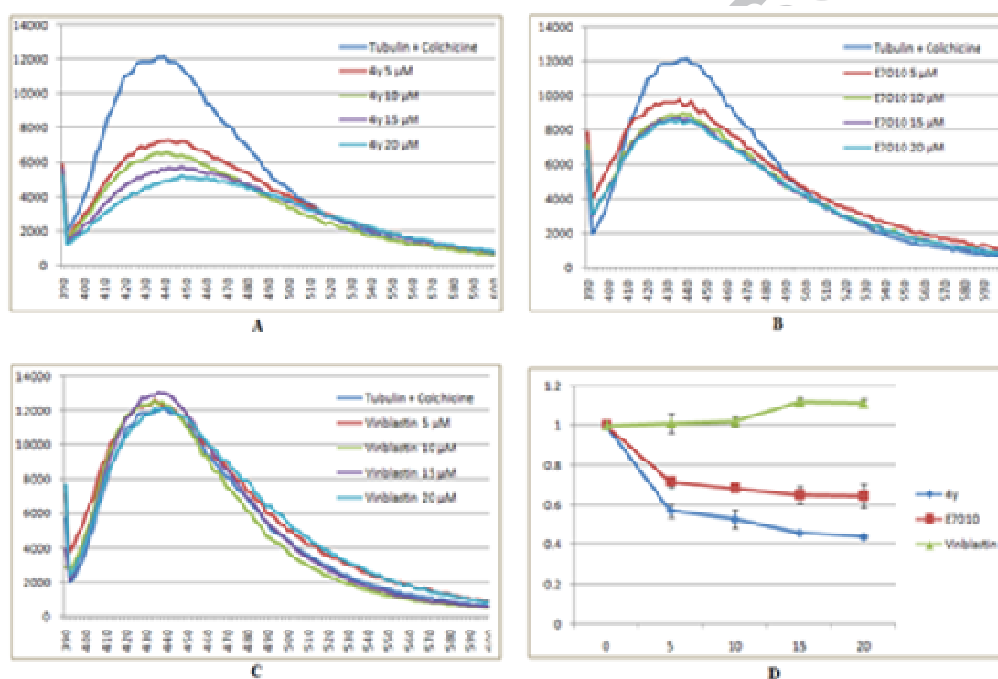


**Figure 5:** Scan of fluorescence wavelength of tubulin colchicine complex coincubated at different concentrations with A) **4y** B) E7010 C) Vinblastine D) Variation of fluorescence of tubulin-colchicine complex observed from Fluorescence based colchicine competitive binding assay of **4y** were carried out at various concentrations containing 3 μM of tubulin and colchicine for 60 min at 37 °C. E7010 was used as a positive control whereas vinblastine was used as negative control which binds at vinca site. Fluorescence values are normalized to DMSO (control).

As discussed previously, molecular modeling studies have been carried out to get an insight into the binding modes of **4y** with tubulin. The protein structure of tubulin was downloaded from protein data bank (PDB code: 3E22) and the docking studies were performed in the colchicine binding domain of tubulin using the software Autodock 4.2. The results suggest that **4y** binds at the interface of  $\alpha$  and  $\beta$  chains of tubulin heterodimer which is depicted in Figure 6A. As evident from the figure several amino acid residues such as Asn 101, Thr 179, Ala 180, Val 181, Asn 249, Ala 250, Leu 252, Arg 253, Lys 254, Leu 255, Lys 352, Thr 353 etc surround **4y** in the binding pocket. A series of hydrophobic interactions have been observed between most of these amino acid residues with aryl and pyridine rings of **4y**. Additionally, two methoxy group of 2-trimethoxyanilinopyridine moiety establishes a hydrogen bonding interaction each with the carboxylate group of the amino acid residue  $\alpha$ Asn 101 (distance 2.9 and 3.3 Å respectively). In the same way, one of the methoxy groups of benzothiazole interacts with the hydroxyl group of  $\beta$ Tyr202. As shown in Figure 6B, the benzothiazole moiety of **4y** is deeply buried in the  $\beta$  subunit of the tubulin while the 2-anilinopyridine moiety is exposed outside towards the  $\alpha$  chain, wherein it establishes several polar and hydrophobic interactions including hydrogen bonding interactions with the surrounding amino acid residues. All these observations illustrate that **4y** exerts a cytotoxic effect by effectively interacting with colchicine binding domain of the tubulin which is evident from the competitive colchicine binding assay.

### 3.4. Molecular modeling studies

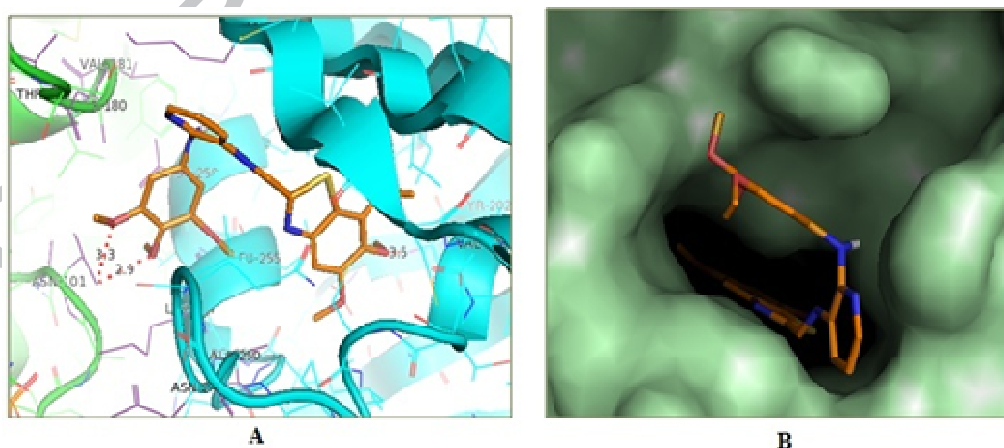


**Figure 6:** A) Binding pose of **4y** (orange) with tubulin.  $\alpha$  and  $\beta$  chains of the protein are colored as green and cyan for better understanding. B) Binding pose of **4y** in  $\beta$  subunit of tubulin.

Drug likeliness properties of the test compound **4y** was carried out using computational approach as described in the experimental section along with E7010. The predicted values of **4y** was compared with the standard E7010 and the values are presented in the Table 3. It was observed that **4y** and E7010 showed resemblance in CYP2C19, CYP2C9, CYP2D6 inhibition and bioavailability score. Both the compounds inhibited the CYP2C9 enzyme with no inhibition of CYP2C19 and CYP2D6 enzymes. Moreover, compound **4y** acted as a weak substrate to CYP3A4 enzyme compared to E7010, which does not act as substrate to this enzyme. Plasma protein binding values of **4y** and E7010 suggested that lower dose of **4y** is required compared to E7010 as blood plasma protein has less bound **4y** compared to E7010. According to the molinspiration calculation both the compounds have comparable bioactive properties with the acceptable limits, such as TPSA values are less than 140 Å, whereas greater than this value may show poor intestinal absorption.<sup>20,21</sup> HIA prediction was important to understand human intestinal absorption of drug, preADMET predictor can be used to identify the percent human intestinal absorption of drug.<sup>22</sup> HIA percentage values of **4y** and E7010 suggested that **4y** has more human intestinal permeability compared to E7010. Further, identification of drug molecule interaction with P-gp protein is an important property for lead optimization. Multi drug resistance (MDR) is also one the major challenge for the new molecules and P-gp, that was identified as one of the main ABC transporter protein responsible for MDR development in cancer cells. To improve the ADMET profile of drug molecules FDA has suggested the importance of finding whether a new molecule is a P-gp substrate or inhibitor. Most of the drug candidates that are identified as P-gp substrate can be readily effluxed, leading to decreased bioavailability in blood plasma.<sup>23-25</sup> *In silico* preADMET prediction showed that **4y** was a P-gp inhibitor, whereas E7010 was neither inhibitor nor substrate. The above ADMET prediction data suggested that the compound **4y** showed moderate to good ADMET properties compared to E7010 which provides further opportunities for the development of similar therapeutic potential derivatives (Table 3).

**Table 3:** ADME properties of the compounds **4y** and E7010 studied by *in silico* preADMET predictor and molinspiration programme.

Properties	E7010	4y
BBB	0.352325	0.477624
CYP_2C19_inhibition	Non	Non
CYP_2C9_inhibition	Inhibitor	Inhibitor
CYP_2D6_inhibition	Non	Non
CYP_2D6_substrate	Non	Non
CYP_3A4_inhibition	Inhibitor	Non
CYP_3A4_substrate	Non	Weakly
HIA	91.716935	98.583151
Pgp_inhibition	Non	Inhibitor
Plasma_Protein_Binding	100	89.509825
Bioavailability Score	0.55	0.55
Rotatable bonds	6	10
H-bond acceptors	5	9
H-bond donors	3	1
miLogP	3.33	4.12
TPSA	100.55	105.58
natoms	26	36
MW	371.42	510.57
nON	7	10
nOHNH	3	1
nviolations	0	1
nrotb	6	10
volume	<b>312.5</b>	<b>442.19</b>

Many anticancer compounds exert their growth inhibitory effect either by arresting the cell cycle at a particular checkpoint or by induction of apoptosis or a combined effect of both cell cycle block and apoptosis.<sup>26</sup> Furthermore regulation of the cell cycle and apoptosis are considered to be effective cancer therapeutic methods.<sup>27</sup> In general, the inhibition of tubulin polymerization is associated with the cell cycle arrest in G2/M phase.<sup>28</sup> Therefore, it was considered of interest to study the cell cycle arrest and the apoptosis inducing ability of compound **4y**. In this investigation, DU-145 cells were treated with compound **4y** at 2.5 and 5  $\mu$ M concentrations along with the reference compound E7010 (5  $\mu$ M) for 48 h. The data

obtained clearly indicated that this compound arrested cell cycle at G2/M phase as compared to the untreated control (Figure 7). The test compound, **4y** showed 37.85 and 66.09 % of cell accumulation in G2/M phase at 2.5 and 5  $\mu$ M concentrations, whereas the reference compound E7010 showed 50.21 % cell accumulation in G2/M phase at 5  $\mu$ M concentration.

### 3.5. Cell cycle analysis

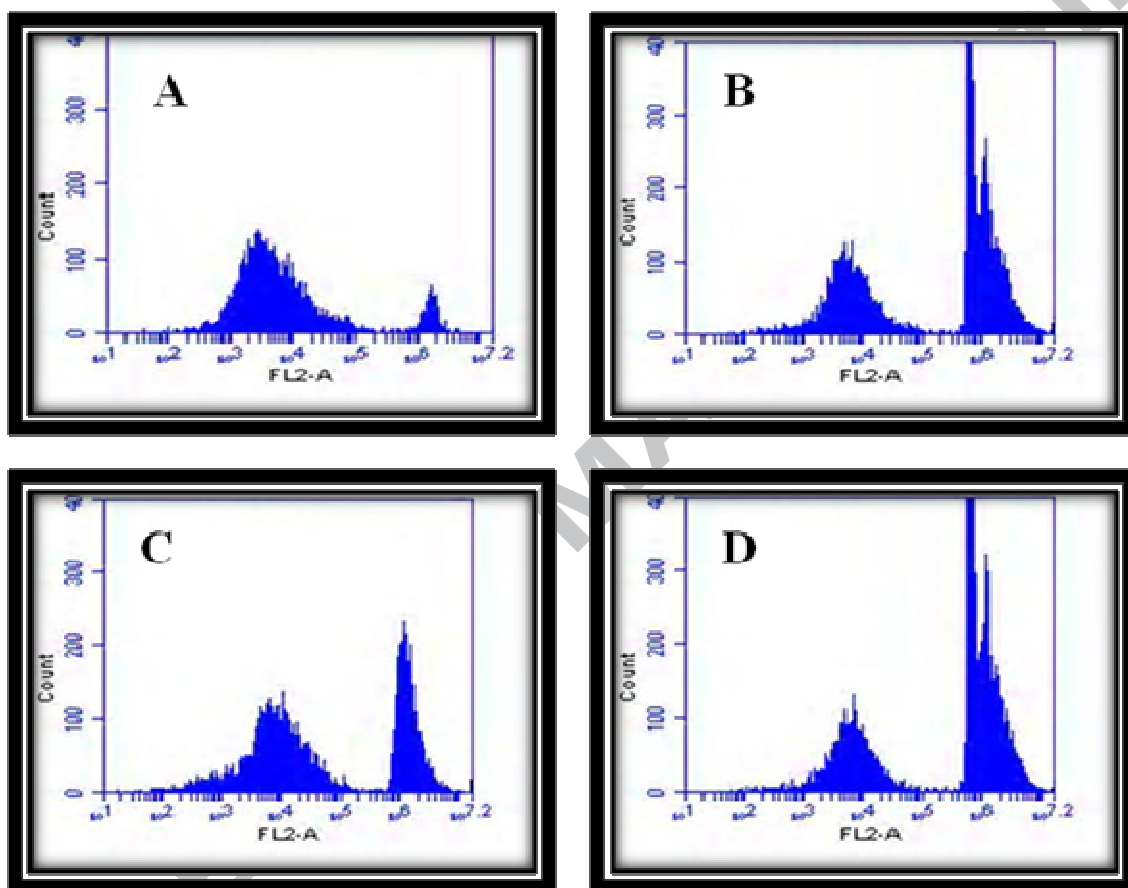


**Figure 7:** Cell cycle distribution in DU-145 cells treated with compound **4y** at 2.5 and 5  $\mu$ M concentrations for 48h. After 48 h of drug treatment with **4y** samples were analyzed by flow cytometry. A: Control cells (DU-145), B: E7010 (5  $\mu$ M), C: **4y** (2.5  $\mu$ M) and D: **4y** (5  $\mu$ M).

**Table 4:** Distribution of DU145 cells in various phases of cell cycle

Sample	Sub G1 %	G0/G1 %	S %	G2/M %
A: Control	0.68	82.09	3.04	11.85
B: E7010 (5 $\mu$ M)	0.42	34.94	0.97	62.59
C: <b>4y</b> (2.5 $\mu$ M)	1.00	55.96	2.52	38.51
D: <b>4y</b> (5 $\mu$ M)	0.46	30.47	0.71	67.56

The maintenance of mitochondrial membrane potential ( $\Delta\Psi_m$ ) is significant for mitochondrial integrity and bioenergetic function.<sup>29</sup> Mitochondrial changes, including loss of mitochondrial membrane potential ( $\Delta\Psi_m$ ), are key events that take place during drug-induced apoptosis. Mitochondrial injury by **4y** was evaluated by detecting drops in mitochondrial membrane potential ( $\Delta\Psi_m$ ). In this study, we investigated the involvement of mitochondria in the induction of apoptosis by compound **4y**. After 48 h of drug treatment with **4y** at 2.5 and 5  $\mu$ M, reduction in mitochondrial membrane potential ( $\Delta\Psi_m$ ) of DU-145 cells was observed which was assessed by JC-1 staining (Figure 8).

### 3.6. Measurement of Mitochondrial Membrane Potential ( $\Delta\Psi_m$ )

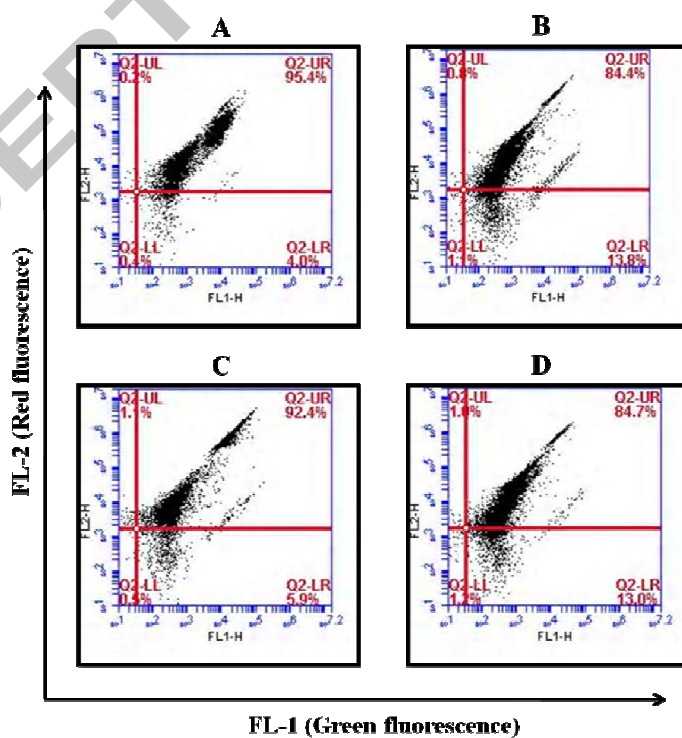


**Figure 8:** Compound **4y** triggers mitochondrial injury. Drops in membrane potential ( $\Delta\Psi_m$ ) was assessed by JC-1 staining of DU-145 cells treated with test compound and samples were then subjected to flow cytometry analysis on a FACScan (Becton Dickinson) in the FL1, FL2 channel to detect mitochondrial potential. Shown are representative dot plots (left panels) and quantification of membrane potential (right panel). A: Untreated control cells (DU-145), B: E7010 (2.5  $\mu$ M), C: **4y** (2.5  $\mu$ M) and D: **4y** (5  $\mu$ M).

The apoptotic effect of compound **4y** was further evaluated by Annexin V FITC/PI (AV/PI) dual staining assay<sup>30</sup> to examine the occurrence of phosphatidylserine externalization and also to understand whether it is due to physiological apoptosis or nonspecific necrosis. In this study, DU-145 cells were treated with compound **4y** for 48 h at 2.5 and 5  $\mu$ M concentrations. It was observed that this compound showed significant apoptosis against DU-145 cells as shown in Figure 9. Results indicated that compound **4y**, showed 16.74 and 25.37 % of apoptosis at 2.5 and 5  $\mu$ M concentrations, respectively whereas the standard E7010 showed 18.26 % of apoptosis at 2.5  $\mu$ M concentration. This experiment suggested that **4y** induced cell death by apoptosis in human prostate cancer cells.

### 3.7. Annexin V-FITC for apoptosis

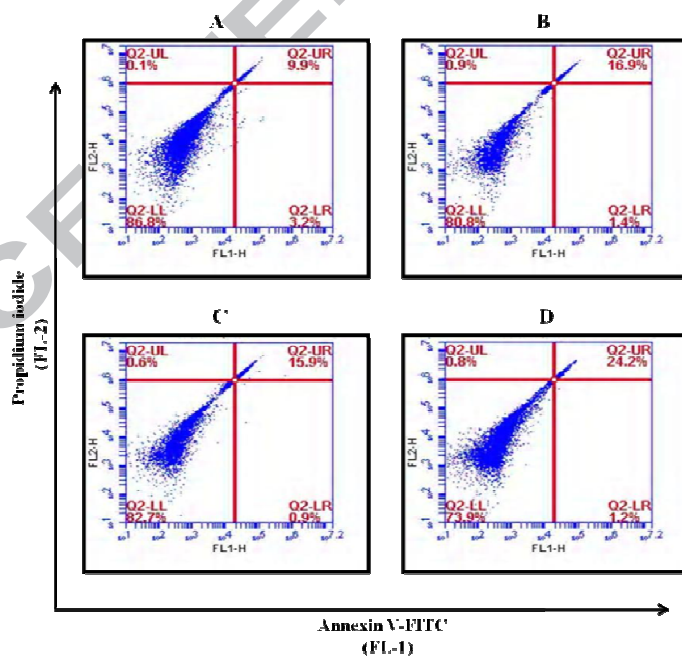


**Figure 9** Annexin V-FITC assay; quadrants represent, lower left (LL) represents live cells, lower right (LR) represents early apoptotic, upper right (UR) represents late apoptotic and upper left (UL) represents necrotic cells. A: Control cells (DU-145), B: E7010 (2.5  $\mu$ M), C: **4y** (2.5  $\mu$ M) and D: **4y** (5  $\mu$ M).

**Table 5:** Distribution of apoptotic cells in Annexin-V FITC experiment

Sample	Upper left %	Upper right %	Lower left %	Lower right %
<b>A: Control (DU-145)</b>	0.14	9.88	86.77	3.21
<b>B: E7010 (2.5 <math>\mu</math>M)</b>	0.93	16.91	80.80	1.35
<b>C: 4y (2.5 <math>\mu</math>M)</b>	0.57	15.88	82.69	0.86
<b>D: 4y (5 <math>\mu</math>M)</b>	0.75	24.21	73.87	1.16

From previous reports, it is well established that molecules affecting microtubule polymerization cause mitotic arrest and ultimately lead to apoptosis.<sup>31</sup> Caspases are a family of cysteine-aspartic proteases that are crucial mediators of apoptosis. Among them, caspase-3 is the best understood in the mammalian caspases in terms of its specificity and role in apoptosis. Furthermore, there are some reports<sup>26</sup> that indicate that the cell cycle arrest at G2/M phase takes place by the induction of cellular apoptosis. Hence, it was considered of interest to understand the correlation of cytotoxicity with apoptosis by **4y**. DU-145 cells were treated with **4y** (2.5 and 5  $\mu$ M) and examined for the activation of caspase-3 activity. Results indicated that there was nearly 1.5 to 2 fold-induction in caspase-3 levels compared to the control (Figure 10).

### 3.8. Effect on activation of caspase 3 activity

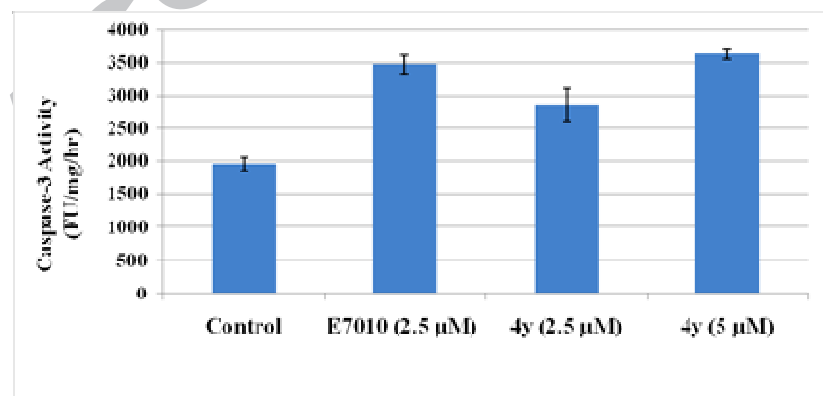


**Figure 10:** Effect of compound **4y** on caspase-3 activity: DU-145 cells were treated with compound **4y** at 2.5 and 5  $\mu$ M concentrations for 48 h. Values indicated are the mean  $\pm$  SD of two different experiments performed in triplicates; \*P < 0.0003, \*\*P < 0.0007, and \*\*\*P < 0.0002 compared to control.

In conclusion, a new molecular structure of Schiff bases resulting from tethering 2-anilinopyridinyl and benzothiazole moieties has been designed by *in silico* molecular modeling technique. The Schiff base with trimethoxy groups on both the moieties **4y** was found to be better than E7010 in binding to the colchicine domain of tubulin, *in silico*. Executing the design, a series of thirty related Schiff bases have been synthesized by diversifying various substituents, both on 2-anilinopyridinyl as well as benzothiazole nucleus. These conjugates were tested for their cytotoxicity against three different human cancer cell lines. Some compounds have shown specificity towards prostate cancer cell line (DU145). Compound **4y** was found to be the potent conjugate from this series exhibiting cytotoxic effects on all the tested cell lines more specifically against DU145 with a GI<sub>50</sub> value of 3.8  $\mu$ M. Moreover, further studies were carried out on **4y** to determine the mechanistic aspects and correlate with the docking results, which indicated that it caused cell cycle arrest in G2/M phase by inhibiting tubulin polymerization. Competitive colchicine binding assay revealed that **4y** competes with colchicine in binding to tubulin. Other detailed biological investigations such as mitochondrial membrane potential, Annexin V-FITC, and caspase-3 assays suggested that this compound significantly triggers the apoptotic cell death.

### Acknowledgements

T.B.S thanks to UKIERI and British Council and S.M.A.H thanks to CSIR, New Delhi for the award of a research fellowship. This work was also supported under the 12<sup>th</sup> Five Year plan project “Affordable Cancer Therapeutics (ACT)” (CSC0301).

## References

1. Perez, E. A. *Mol. Cancer Ther.* **2009**, *8*, 2086.
2. Zhou, J.; Yao, J.; Joshi, H. J. *Cell Science.* **2002**, *115*, 3547.
3. a) Jordan, M. A.; Wilson, L. *Nat. Rev. Cancer.* **2004**, *4*, 253; b) Kingston, D. G. I. J. *Nat. Prod.* **2009**, *72*, 507.
4. a) Schwartz, E. L. *Clin Cancer Res.* **2009**, *15*, 2594.; b) Pasquier, E.; Andrè, N.; Braguer, D. *Curr. Cancer Drug Targets.* **2007**, *7*, 566.
5. Lu, Y.; Chen, J.; Xiao, M.; Li, W.; Miller, D. D. *Pharm. Res.* **2012**, *29*, 2943.
6. Yokoi, A.; Kuromitsu, J.; Kawai, T.; Nagasu, T.; Sugi, N. H.; Yoshimatsu, K.; Yoshino, H.; Owa, T. *Mol. Cancer Ther.* **2002**, *1*, 275.
7. a) Solomon, V. R.; Hu, C.; Lee, H. *Bioorg. Med. Chem.* **2009**, *17*, 7585; b) Hutchinson, I.; Jennings, S. A.; Vishnuvajjala, B. R.; Westwell, A. D.; Stevens, M. F. *J. Med. Chem.* **2002**, *45*, 744.
8. Prota, A.E.; Bargsten, K.; Diaz, J.F.; Marsh, M.; Cuevas, C.; Liniger, M.; Neuhaus, C.; Andreu, J.M.; Altmann, K.H.; Steinmetz, M.O. *Proc Natl Acad Sci U S A.* **2014**, *111*, 13817.
9. a) Kamal, A.; Hussaini, S. M. A.; Nayak, V. L.; Malik, M. S.; Sucharitha, M. L.; Shaik, T. B.; Ashraf, M.; Bagul, C. *Bioorg. Med. Chem.* **2014**, *22*, 6755; b) Kamal, A.; Reddy, N. V. S.; Nayak, V. L.; Bolla, N. R.; Rao, A. V. S.; Prasad, B. *Bioorg. Med. Chem.* **2014**, *22*, 3465; c) Kamal, A.; Khan, M. N. A.; Reddy, K. S.; Rohini, K. *Bioorg. Med. Chem.* **2007**, *15*, 1004.
10. a) Kamal, A.; Sultana, F.; Ramaiah, M. J.; Srikanth, Y. V. V.; Viswanath, A.; Kishor, C.; Sharma, P.; Pushpavalli, S. N. C. V. L.; Addlagatta, A.; Pal-Bhadra, M. *Chem.Med.Chem.* **2012**, *7*, 292; b) Kamal, A.; Mallareddy, A.; Suresh, P.; Shaik, T. B.; Nayak, V. L.; Kishore, C.; Shetti, R. V. C. R. N. C.; Rao, N. S.; Tamboli, J. R.; Ramakrishna, S.; Addlagatta, A. *Bioorg. Med. Chem.* **2012**, *20*, 3480.
11. Sztanke, K.; Maziarka, A.; Osinka, A.; Sztanke, M. *Bioorg. Med. Chem.* **2013**, *21*, 3648.
12. Kamal, A.; Ashraf, M.; Vishnu Vardhan, M. V. P. S.; Faazil, S.; Nayak, V. L. *Bioorg. Med. Chem. Lett.* **2014**, *24*, 147.

13. Kamal, A.; Srikanth, Y. V. V.; Shaik, T. B.; Khan, M. N. A.; Ashraf, M.; Reddy, M. K.; Kumar, K. A.; Kalivendi, S. V. *Med. Chem. Commun.* **2011**, *2*, 819.
14. Kamal, A.; Srikanth, Y. V. V.; Khan, M. N. A.; Ashraf, M.; Reddy, M. K.; Sultana, F.; Kaur, T.; Chashoo, G.; Suri, N.; Sehar, I.; Wani, Z. A.; Saxena, A.; Sharma, P. R.; Bhushan, S.; Mondhe, D. M.; Saxena, A. K. *Bioorg. Med. Chem.* **2011**, *19*, 7136.
15. Negi, A. S.; Gautam, Y.; Alam, S.; Chanda, D.; Luqman, S.; Sarkar, J.; Khan, F.; Konwar, R. *Bioorg. Med. Chem.* **2015**, *23*, 373.
16. Cormier, A.; Marchand, M.; Ravelli, R. B. G.; Knossow, M.; Gigant, B. *EMBO Rep.* **2008**, *9*, 1101; b) Morris, G. M.; Huey, R.; Lindstrom, W.; Sanner, M. F.; Belew, R. K.; Goodsell, D. S.; Olson, A. J. J. *Comput. Chem.* **2009**, *16*, 2785.  
<http://autodock.scripps.edu/>.
17. Huber, K.; Patel, P.; Zhang, L.; Evans, H.; Westwell, A. D.; Fischer, P. M.; Chan, S.; Martin, S. *Mol. Cancer Ther.* **2008**, *7*, 143.
18. a) Kamal, A.; Balakrishnan, G.; Ramakrishna, G.; Shaik, T. B.; Sreekanth, K.; Balakrishna, M.; Rajender, Dastagiri, D.; Kalivendi, S. V. *Eur J Med Chem.* **2010**, *45*, 3870.  
b) Larocque, K.; Ovadje, P.; Djurdjevic, S.; Mehdi, M.; Green, J.; Pandey, S. *PloS one.* **2014**, *9*, e87064.
19. Bhattacharyya, B.; Wolff, J. *PNAS-USA.* **1974**, *71*, 2627.
20. Tanwara O.P.; Sahaa, R.; Marellaa, A.; Alama, M.M.; Akhtera, M.; Kumar, D.V. *Journal of Advanced Bioinformatics Applications and Research.* **2014**, *5*, 172-182.
21. Kovačević, SZ.; Jevrić, LR.; Kuzmanović, SO.; Lončar, ES. *Iranian journal of pharmaceutical research: IJPR.* **2014**, *13*, 899.
22. Nerkar, AG.; Kudale, SA.; Joshi, PP.; Chikhale, HU. *Int J Pharm Pharm Sci.* **2012**, *4*, 449-53.
23. Poongavanam, V.; Haider, N.; Ecker, GF. *Bioorganic & medicinal chemistry.* **2012**, *20*, 5388-95.
24. Li, D.; Chen, L.; Li, Y.; Tian, S.; Sun, H.; Hou, T. *Molecular pharmaceutics.* **2014**, *11*, 716-26.
25. Srivalli, KM.; Lakshmi, PK. *Brazilian Journal of Pharmaceutical Sciences.* **2012**, *48*, 353-67.

26. Liu, Z.; Zhou, Z.; Tian, W.; Fan, X.; Xue, D.; Yu, L.; Yu, Q.; Long, Y.-Q. *Chem.Med.Chem.* **2012**, *7*, 680.
27. Chan, K. T.; Meng, F. Y.; Li, Q.; Ho, C. Y.; Lam, T. S.; To, Y.; Lee, W. H.; Li, M.; Chu, K. H.; Toh, M. *Cancer Lett.* **2010**, *294*, 24-118; b) J. K. Shen, H. P. Du, M. Yang, Y. G. Wang, J. Jin, *Ann. Hematol.* **2009**, *88*, 743-752.
28. Blank, M.; Shiloh, Y.; *Cell Cycle.* **2007**, *6*, 686.
29. Budihardjo, I.; Oliver, H.; Lutter, M.; Luo, X.; Wang, X. *Annu. Rev. Cell Dev. Biol.* **1999**, *15*, 269.
30. (a) Hengartner, M. O. *Nature* **2000**, *407*, 770. (b) Sun, S.-Y.; Hail, N., Jr.; Lotan, R. J. *Natl. Cancer Inst.* **2004**, *96*, 662
31. Weir, N. M.; Selvendiran, K.; Kutala, V. K.; Tong, L.; Vishwanath, S.; Rajaram, M.; Tridandapani, S.; Anant, S.; Kuppusamy, P. *Cancer Biol. Ther.* **2007**, *6*, 178.
32. Zhang, L. H.; Wu, L.; Raymon, H. K.; Chen, R. S.; Corral, L.; Shirley, M. A.; Narla, R. K.; Gamez, J.; Muller, G. W.; Stirling, D. I.; Bartlett, B. J.; Schafer, P. H.; Payvandi, F. *Cancer Res.* **2006**, *66*, 951.

## Graphical Abstract

